International Journal of Hydrogen Energy xxx (xxxx) xxx

Contents lists available at ScienceDirect

International Journal of Hydrogen Energy

journal homepage: www.elsevier.com/locate/he

A techno-economic and environmental evaluation of the integration of direct air capture with hydrogen derivatives production

Enric Prats-Salvado [a,b,*], Nathalie Monnerie [a], Christian Sattler [a,b]

[a] German Aerospace Center (DLR), Institute of Future Fuels, Linder Höhe, Cologne, Germany
[b] RWTH Aachen University, Chair for Solar Fuel Production, Templergraben 55, Aachen, Germany

ARTICLE INFO

Handling Editor: Ibrahim Dincer

ABSTRACT

Carbon-neutral fuels are key to decarbonizing hard-to-abate sectors. Solar redox cycles can produce them by creating oxygen vacancies in a metal oxide capable of splitting water and CO_2. The resulting synthesis gas can be processed into a liquid fuel like methanol. To close the carbon cycle, feedstock CO_2 can be captured from the atmosphere with direct air capture (DAC), but the synergies between synthetic fuel production and DAC are largely unexplored. In this work, four integration strategies between DAC and solar redox cycles are proposed. Each of them is modeled with Aspen Plus and HFLCAL and compared with a techno-economic and a cradle-to-gate life cycle assessment. The optimal configuration, with a levelized cost of 7.9 ± 0.4 $USD_{2022}/kg_{Methanol}$ and a climate change impact of -450 ± 30 g $CO_2e/kg_{Methanol}$, uses solid DAC powered by waste heat. Therefore, the study recommends the integration of DAC in the production of synthetic fuels.

1. Introduction

Without action, global temperatures could rise by 2.7 °C by 2100, disrupting nearly every ecosystem in the world [1,2]. Tackling climate change will involve transitioning away from fossil fuels, which in turn calls for a major technological breakthrough [3,4]. Here, two important technologies that can foster the energy transition are explored: direct air capture of CO_2 and solar thermochemical cycles.

Direct air capture of CO_2 (DAC) has attracted considerable attention in recent years due to its ability to remove and concentrate very dilute carbon dioxide from the atmosphere. The removed CO_2 can either be sequestered or used as a feedstock for the carbon capture and utilization industry (CCU) [5]. While relatively expensive compared to other capture technologies, DAC differs from other alternatives in that it does not have obvious biophysical limitations (as biogenic sources do) and can produce truly carbon-neutral CO_2 when powered by renewable energy (as opposed to point-source carbon capture of industrial flue gases, which contain mostly fossil CO_2) [6–8]. One of the most pressing concerns surrounding the proliferation of DAC is its high energy consumption. Furthermore, the energy utilized must be as low-carbon as possible to prevent a drastic reduction in system efficiency due to the associated indirect emissions [9–11]. As a consequence, there is a need for technological developments that can address this issue [12]. At the present time, there is a broad portfolio of DAC technologies. Two of these are considered in this study on the basis of their superior readiness, namely solid sorbent and liquid solvent direct air capture, frequently referred to simply as S-DAC and L-DAC, respectively. While S-DAC employs a solid sorbent that adsorbs carbon dioxide, the L-DAC process relies on a liquid solvent that chemically absorbs the CO_2 in the air. Notably, the former can release the captured carbon dioxide by applying heat at low temperatures (around 100 °C), while the latter requires elevated temperatures for regeneration (as high as 900 °C), for which oxyfuel combustion of natural gas is often proposed, resulting in the mixing of fossil CO_2 with atmospheric CO_2 [5,13,14]. Solar thermochemical cycles, unlike the currently most mature processes that rely on electricity, can produce hydrogen directly from heat. This avoids the energy losses involved in power generation and greatly increases the potential efficiency of the technology [15–17]. There are several types of solar thermochemical cycles. Here, the focus is on a technology called redox cycles, where a metal oxide (in this case, cerium dioxide) is reduced at elevated temperatures and low oxygen partial pressures to form oxygen vacancies in the metal oxide structure. The material is then oxidized again in the presence of steam at lower temperatures to produce hydrogen. This process can also occur in the presence of CO_2, resulting in the formation of carbon monoxide, which can be combined with hydrogen to produce synthetic liquid fuels [18,19]. The reactions

* Corresponding author. German Aerospace Center (DLR), Institute of Future Fuels, Linder Höhe, Cologne, Germany.
E-mail address: enric.pratssalvado@dlr.de (E. Prats-Salvado).

https://doi.org/10.1016/j.ijhydene.2024.10.026
Received 14 June 2024; Received in revised form 20 September 2024; Accepted 3 October 2024

do not consume any metal oxide and the cycle can start again with the reduction step [20,21]. It is nevertheless important to note that, at the time of writing, the efficiency of redox cycles remains relatively low in comparison to other synthetic fuel production pathways [22]. Indeed, the most efficient reactor is only able to store 5.25% of the solar energy supplied to the reactor as fuel, and when accounting for the DAC unit or the downstream processing, the efficiency is reduced even further [23]. Although there are several promising designs and strategies that could substantially enhance the technology's performance in the near future [24–26], the utilization of the available waste heat for powering often overlooked side-processes, such as the CO_2 supply, represents an indirect way of increasing the overall system efficiency [27]. Currently, the most significant legislative instruments on low-carbon fuels permit the utilization of CO_2 from point source carbon capture as a feedstock for hydrogen-derived liquid fuels. However, DAC (and equivalent processes that capture atmospheric CO_2) are the only possible sources to produce carbon-neutral synthetic fuels [28–31], which makes the integration of DAC and the production of synthetic fuels a promising area of research. Recent studies in the field of green methanol production have included the DAC units within their boundaries. Nevertheless, existing research either excludes integration between fuel production and the DAC system [31–33] or, when integration is considered, details regarding the benefits of this integration are not provided [34,35]. This work attempts to address this knowledge gap by quantifying the significance of integrating DAC with fuel production, using solar redox cycles as a case study. This research builds on previous studies published by the authors, in which the different synergies were identified, modeled, and evaluated from a techno-economic perspective [27,36]. Herein, the final results are reported, merging the environmental with an updated economic assessment that provides a more realistic cost estimation.

The study comprises a description of the various proposed integration strategies, followed by a methodology section in which the details and assumptions utilized in the modeling and economic and environmental assessments are documented. Then, the economic and carbon footprint results are presented, accompanied by their respective breakdowns, a sensitivity analysis, and a discussion of the burden shifting between impact categories. Finally, the levelized cost and the carbon footprint of the produced methanol are combined and compared to fossil methanol.

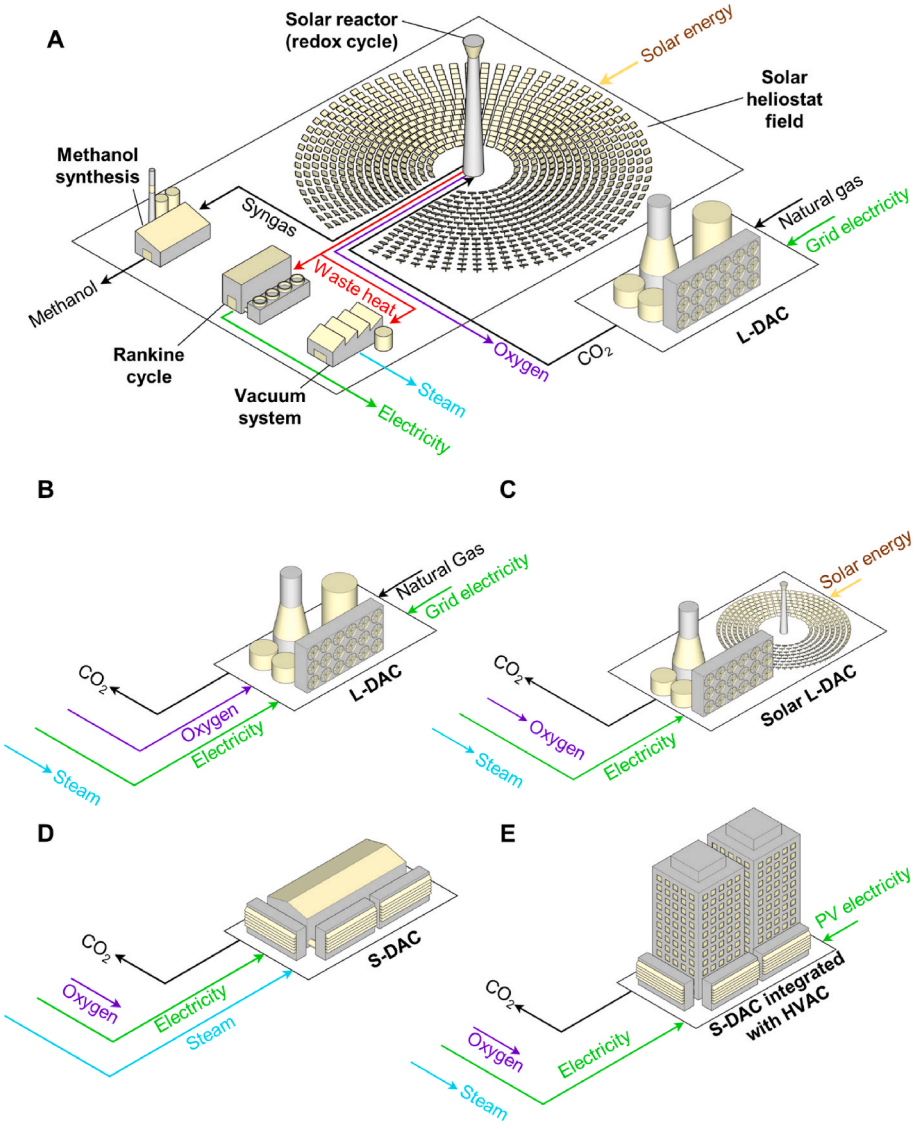

Fig. 1. Overview of the scenarios considered in this study, which involve the integration of solar methanol production by a redox thermochemical cycle with different DAC technologies. At the top of figure (A), a complete system-level flowsheet diagram is shown for the baseline case. For the sake of simplicity, the remaining diagrams have omitted the fuel production section, as it remains unchanged. These diagrams illustrate the integration strategies for the "L-DAC + O_2" scenario (B), the "L-DAC + Solar" scenario (C), the "S-DAC + Steam" scenario (D) and the "S-DAC + HVAC" scenario (E).

2. Material and methods

As illustrated in Fig. 1, four distinct scenarios were developed, each with a unique configuration integrating DAC with the solar thermochemical cycle [27,36]. These scenarios were then evaluated against a baseline with no integration between DAC and the solar fuel production. The baseline scenario considers conventional L-DAC due to the generally higher maturity of the different units that comprise it, although its technology readiness level (TRL) is in practice comparable to that of S-DAC [37].

In the "L-DAC + O_2" scenario, the conventional L-DAC with oxyfuel natural gas combustion is also considered, but it utilizes the oxygen produced by the thermochemical cycle instead of relying on an air separation unit. The "L-DAC + Solar" scenario introduces a new concept where L-DAC is powered entirely by solar energy, eliminating the need for oxyfuel natural gas combustion. The "S-DAC + Steam" scenario features an S-DAC system installed in the solar fuel plant, capable of utilizing low-quality waste heat in the form of low-pressure steam from the thermochemical cycle. Finally, the "S-DAC + HVAC" scenario involves a decentralized S-DAC system, capturing CO_2 from the airflow in the heating, ventilation, and air conditioning (HVAC) systems of buildings in urban areas near the plant [38].

It should be noted that the four scenarios presented do not represent all possible combinations (which increase substantially when including emerging DAC technologies or small-scale systems), but they provide an overview of the simplest combinations for the most mature DAC technologies. It is also important to note that in configurations where natural gas is burned in the L-DAC, only the fraction of atmospheric CO_2 is used as feedstock, while the fossil fraction is permanently sequestered.

As observed in Fig. 1, surplus electricity generated in the thermochemical cycle is utilized in the DAC units for all integration scenarios. Nevertheless, some of them, namely "L-DAC + O_2" and "S-DAC + HVAC", necessitate supplementary electricity input. In the case of the former, this input is required on a continuous basis, thus considering grid electricity from a pricing and emissions perspective. For the latter, since electricity input is only needed during the day, cheaper and greener electricity produced with photovoltaics (PV) was considered.

Simulations were developed for each component of the process. The models for the conventional L-DAC and S-DAC were extracted from literature [39,40]. In the case of the conventional L-DAC, the model had to be adapted to consider the impact of environmental factors (i.e., temperature, relative humidity and atmospheric pressure) [41]. For the solar L-DAC, the Aspen Plus® and HFLCAL models developed in a dedicated study previously published by the authors were utilized [42].

The fuel production process, consisting of the thermochemical cycle, methanol synthesis, and auxiliary systems (e.g., vacuum system and Rankine cycle), is shown in Fig. 2. This process was modeled in Aspen Plus®, while the heliostat field and solar tower were simulated with the DLR software HFLCAL [43]. Further details regarding these simulations can be found in the Supplementary Information.

For the redox thermochemical cycle, a particle reactor was considered to reduce CeO_2 at 1500 °C and 1 mbar under design conditions, which translates into a reduction extent (δ_{red}) of 0.0221 [44]. Afterwards, these particles were split into two branches to perform the carbon dioxide and water splitting in dedicated oxidation reactors at 900 °C and 1 bar. Under these conditions, a conversion of steam and CO_2 of 40% is expected [44].

Due to the large temperature difference between the reduction and oxidation reactors, heat transfer between hot and cold particles streams is desirable. While there are several approaches being studied about the most efficient way to perform this heat recovery, a set of indirect heat exchangers with supercritical CO_2 as a heat transfer fluid was considered in this work based on literature recommendations [45–47]. The system achieves a heat transfer of 50% between hot and cold particle streams and uses the remaining heat for two purposes: preheating water and CO_2 to 900 °C before being fed to the oxidation reactors and producing motive steam for the vacuum system.

As extensively described in literature, low oxygen partial pressure at

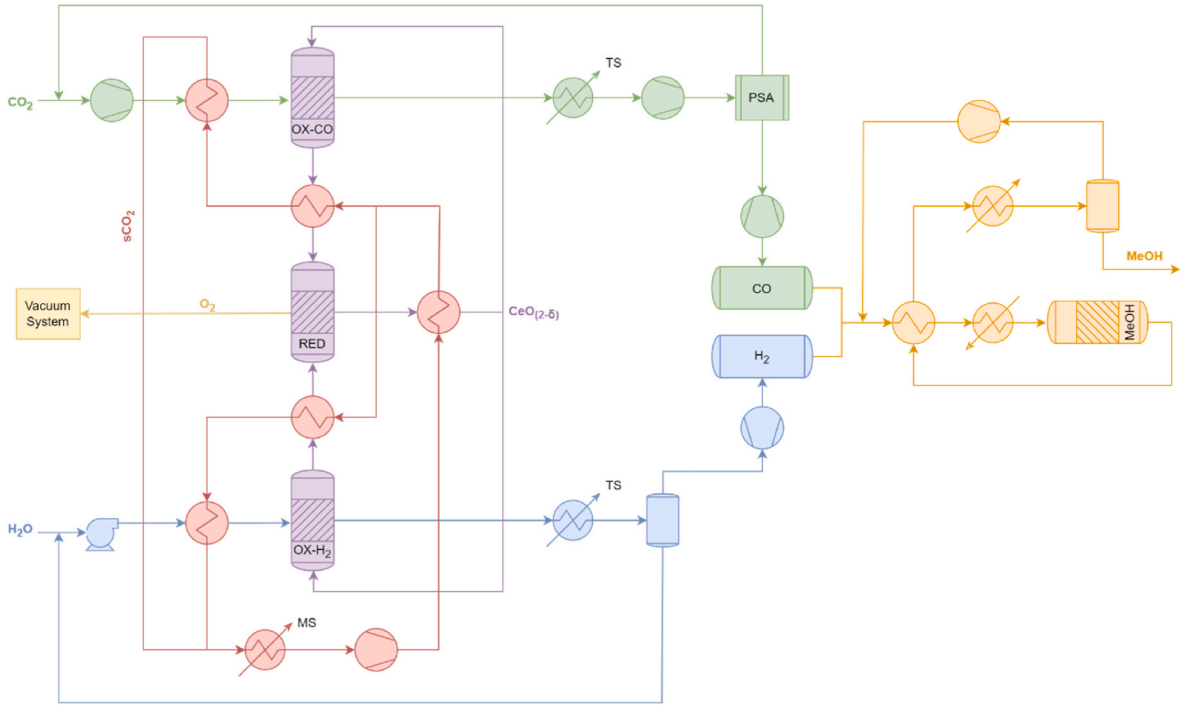

Fig. 2. Simplified process flow diagram of the solar fuel production system. The different colors used in the diagram describe the stream compositions: blue for H_2O/H_2, green for CO_2/CO, purple for $CeO_{(2-\delta)}$, red for supercritical CO_2 (shown as "sCO_2"), orange for CO/H_2/methanol (the latter shown as "MeOH") and yellow for O_2. Additionally, the type of steam produced is shown next to the main heat exchangers used for steam generation: "MS" stands for motive steam and is used in the vacuum system, and "TS" stands for turbine steam and used in the Rankine cycle. (For interpretation of the references to color in this figure legend, the reader is referred to the Web version of this article.)

the reduction reactor increases the metal oxide's reduction extend, thus improving the overall efficiency of the system [44]. While this low oxygen partial pressure can also be achieved by a sweep gas (such as nitrogen or argon), vacuum has been reported to be more energy efficient [48]. In the present work, vacuum produced with multiple stages of steam jets was considered. Although steam jets may not be the most efficient systems, their low cost combined with the availability of large quantities of motive steam makes them especially suitable for oxygen pumping in redox thermochemical cycles [49]. Since the fuel production was forced to be energetically autonomous (i.e., without additional power input to operate the vacuum system), the vacuum level was dependent on the amount of waste heat available as motive steam. This constraint set the reduction pressure of the reduction at 1 mbar, as operating the system at a lower pressure (e.g., 0.5 mbar) would result in a higher reduction extent, which, for a given plant capacity, would translate into a lower ceria flow rate. Consequently, a lower motive steam flow rate would be available, which would be insufficient to sustain the higher energy demand of the new vacuum [36].

The reactor operating conditions for the methanol synthesis were set at 250 °C and 50 bar with a synthesis gas conversion of 50%. Isothermal operation was assumed with the heat generated being removed by a cooling jacket that produces steam [50]. For simplicity, the reaction kinetics were not implemented in the reactor model. Due to this simplification, parallel reactions that would actually occur due to CO_2 impurities in the feed were not considered. The methanol production was assumed to be continuous as opposed to the intermittent synthesis gas production via the redox cycle. This choice aims to reduce the investment cost of the methanol plant due to the much higher number of full load hours, but it requires a storage system for the produced hydrogen and carbon monoxide as a buffer. This storage was designed at 50 bar and sized to supply the methanol plant for 48 h.

In alignment with other green methanol projects, a net capacity of 10 kt of methanol per year was assumed considering a utilization rate of 90% [51]. To achieve this capacity, the optimal solar field size was found to provide 400 MW of thermal power under design conditions. This is a trade-off between a small solar field that is too close to the nominal capacity of the redox cycle (resulting in a low number of full-load hours of the chemical equipment) and an oversized solar field that wastes large amounts of solar energy through curtailment during the annual peak hours. In order to reach the desired temperatures, the solar flux was set at 2.5 MW/m^2 [26,52]. These conditions cause the reactor to have a steady-state efficiency of 73.1% when considering the reflectivity, reradiation and convection losses [53,54]. In total, the solar field had 6345 heliostats (with a combined reflective area of 1.42 km^2) and a 250-m tower, in line with the towers built for the largest concentrating solar power (CSP) projects in existence today [55]. Apart from recommending the optimal solar field layout, the HFLCAL software also provided the solar field efficiencies depending on the solar elevation and azimuth angles, which can be found in the Supplementary Information.

The location selected for the study was an extensive plot of undeveloped land near the city of Riyadh, Saudi Arabia, with approximate coordinates of 25°N and 47°E and an altitude of 695 m above the sea level. The developed model considered the locally available solar irradiance, temperature, relative humidity and atmospheric pressure. These data were provided with hourly resolution by Meteonorm® software.

While the focus of this work is performing a techno-economic and environmental assessment, the solar-to-fuel efficiency of the system is also used for discussing the results. This efficiency is generally expressed as the ratio of the energy content of the synthetic fuel produced (considering the higher heating value or HHV) to the total primary energy input to the system. Since the process uses renewable energy that varies over time, system efficiency (η_{System}) is dynamic. For this reason, the efficiency calculation is on a yearly basis as shown in Eq. (1) and Eq. (2) [27] (where $\dot{m}$ and A stand for mass flowrate and area, respectively).

For some scenarios, an additional input of auxiliary energy ($\dot{Q}_{Auxiliary}$) has to be considered in case of using natural gas or grid electricity ($\dot{W}$). The former was calculated as the annual consumption of natural gas multiplied by its lower heating value (LHV), since the calciner in the L-DAC process cannot use the water evaporation enthalpy. The latter is calculated as the annual electricity consumption divided by an estimated efficiency of 20% (η_{CSP}) to convert it to primary energy assuming that is produced by CSP [56].

$$\eta_{System} = \frac{\dot{m}_{Methanol\ Annual} \bullet HHV_{Methanol}}{DNI_{Annual} \bullet A_{Field} + \dot{Q}_{Auxiliary}} \quad \text{Eq. 1}$$

$$\dot{Q}_{Auxiliary} = \dot{m}_{Natural\ Gas\ Annual} \bullet LHV_{Natural\ Gas} + \frac{\dot{W}_{Electricity\ Annual}}{\eta_{CSP}} \quad \text{Eq. 2}$$

Capital expenditure (CAPEX) was calculated using the results of the simulations and a combination of available correlations for mature process equipment [57] and cost estimation techniques from existing studies for non-standard units [58]. In addition, the operational expenditure (OPEX) was determined by considering fixed (i.e., maintenance) and variable costs (i.e., raw materials, utilities and labor). The equations and data used to calculate the CAPEX and OPEX can be found in the Supplementary Information.

The levelized cost of fuel (LCOF) was calculated from the annualized CAPEX, assuming local WACC as the discount rate (i.e. 6.8% [59]) and a 25-year operating life, the OPEX, and by-product revenues. To determine the uncertainty of the results, the standard deviation of the final CAPEX was extracted from a 1000-sample Monte Carlo simulation by assigning a confidence interval of 30 and 50% to the costs of high- (TRL of 9) and low-maturity units (TRL 6–8), respectively.

The environmental impact of the methanol produced was analyzed using a life cycle assessment (LCA). As in the TEA, the functional unit for all scenarios and the baseline is 1 kg of crude methanol. The boundaries of the LCA are cradle-to-gate because the final product is a synthetic fuel with exactly the same structure and characteristics as its fossil counterpart, and therefore the transport, use and end-of-life phases can be considered equivalent. The LCA was performed with openLCA 2.0.0 and the EcoInvent 3.7.1 database. The selected impact assessment method is "ReCiPe Midpoint (H) w/o LT" [60]. Since the main motivation for using synthetic fuels produced from atmospheric CO_2 is their much lower carbon footprint, the main midpoint environmental impact category reported in the results section is "climate change", expressed in terms of the equivalent mass of CO_2 emitted into the atmosphere (kg CO_2e). However, the other categories are also analyzed and the potential burden shifting between categories will be discussed.

The life cycle inventory (LCI) for each scenario was compiled using the available information from the models developed for solar fuel production and DAC. These models allow an easy estimation of the inputs and outputs of the system in terms of feedstock, utilities and waste. Fugitive emissions were assumed to be 2% of the methanol produced, based on literature recommendations [61], while emissions from intermediates were considered negligible. The infrastructure required to produce the solar fuel was incorporated in several ways. For the L-DAC and S-DAC, an existing LCA in the literature was used for the inventory of construction materials [7]. The solar L-DAC, however, required the creation of its own inventory by adapting the LCA used for L-DAC [42]. For the solar field, the redox cycle and its auxiliary equipment, different parts of the CSP plant available in the Ecoinvent database were used as proxies [62]. A figure illustrating the LCA boundaries, the description of the proxies and the complete LCI for each scenario can be found in the Supplementary Information.

3. Results and discussion

The main results of the techno-economic assessment are shown in Fig. 3. All integrated scenarios demonstrate a cost reduction compared

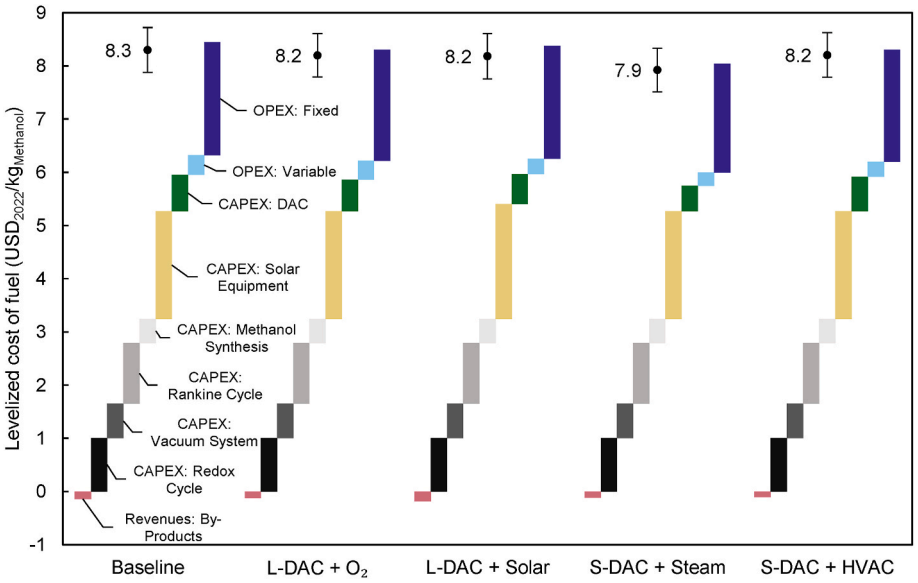

Fig. 3. Levelized cost of fuel (LCOF) and its uncertainty (shown as black dots) accompanied by its breakdown (shown in bars) for the methanol produced in each scenario. The categories common to all scenarios are shown in greyscale. The terms "CAPEX", "OPEX" and "DAC" stand for capital expenditure, operational expenditure and direct air capture, respectively.

to the baseline LCOF. The most cost-effective integration is the "S-DAC + Steam" scenario, which benefits from both the lowest DAC CAPEX and the lowest variable OPEX.

The reduced CAPEX in the "S-DAC + Steam" scenario can be attributed to the scaling of costs for S-DAC. In large-scale S-DAC facilities, CAPEX is primarily driven by the adsorbent, while the process equipment represents a smaller share [14]. However, for the relatively small S-DAC plant required to supply the methanol production in this study, the adsorbent costs scale linearly with the amount of CO_2 captured, while the scaling factors for process equipment are adjusted based on specific types of equipment [58]. Consequently, the S-DAC has a CAPEX advantage over the L-DAC, which consists primarily of process equipment.

The ability of S-DAC to utilize large amounts of waste heat from the fuel production process is particularly advantageous, resulting in the lowest variable OPEX. The other scenarios do not achieve a comparable level of energy integration and incur higher CAPEX at this plant scale. Although the "S-DAC + HVAC" scenario uses the same DAC technology as the "S-DAC + Steam" scenario, the CAPEX associated with the DAC is the second highest after the baseline. This is due to the need to install multiple smaller units in different buildings.

Moreover, a sensitivity analysis was conducted to assess the impact of some variables on the LCOF. For this analysis, the scenario with the lowest LCOF was chosen ("S-DAC + Steam"), the most insightful variables were selected, and reasonable ranks were suggested for each of them. The results are displayed in Fig. 4. The economics are strongly

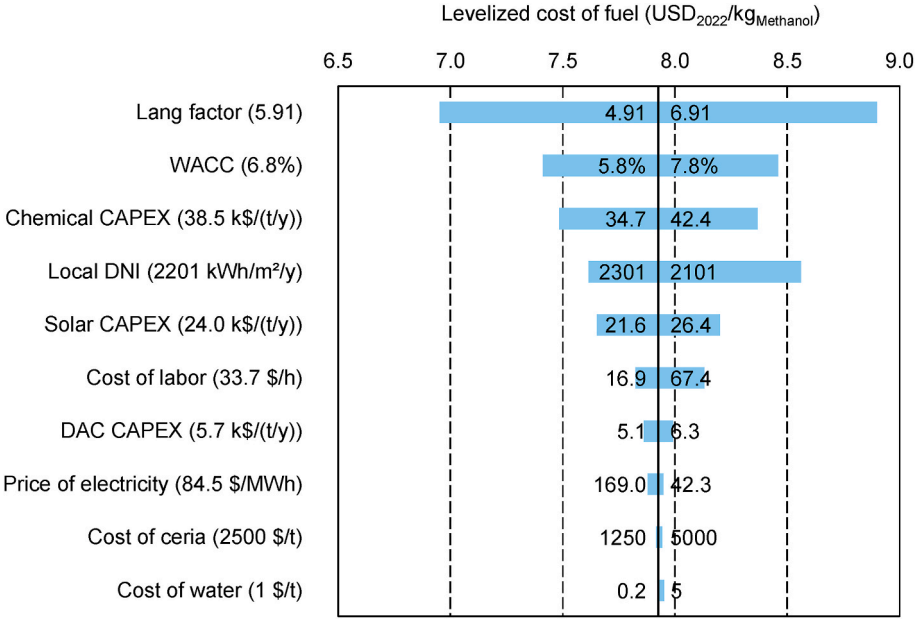

Fig. 4. Sensitivity analysis results for the "S-DAC + Steam" scenario, which has the lowest levelized cost of fuel. The original value in the techno-economic assessment is shown in parentheses next to each variable name. The terms "CAPEX", "WACC" and "DNI" stand for capital expenditure, weighted average cost of capital and direct normal irradiance, respectively. All costs are expressed in USD_{2022}.

influenced by the Lang factor, which could be reduced as the technology develops. The location also plays an important role, as the DNI and the WACC have a significant impact. As already observed in Fig. 3, the largest contributor to the CAPEX of the system is the chemical process equipment (i.e. the combination of redox cycle, vacuum system, Rankine cycle and methanol system).

The results of the LCA in Fig. 5 show that the integrations applied to each scenario resulted in significant greenhouse gas (GHG) emission savings compared to the baseline. In addition, an LCA was performed for 1 kg of methanol produced from natural gas in order to have a fossil benchmark. As expected, the cradle-to-gate carbon footprint for the solar methanol was much lower than for the fossil alternative. It is also noteworthy that the cradle-to-gate GHG emissions for solar methanol are negative because, within the battery limits of the plant, the atmospheric CO_2 can be considered to be stored in the methanol. However, solar methanol produced with CO_2 from DAC, similar to any other CCU fuel, should not be understood as a carbon capture and storage (CCS) solution (i.e., a process whose ultimate goal is to store CO_2, thus resulting in negative emissions) [63]. As presented, the scenario with the lowest cradle-to-gate carbon footprint is the "S-DAC + Steam" scenario, followed by the "L-DAC + Solar". The differences between the scenarios are much more pronounced in the environmental evaluation than in the techno-economic evaluation. This is because while LCOF is dominated by CAPEX (and fixed OPEX, which is directly dependent on CAPEX), the cradle-to-gate carbon footprint is much more related to aspects such as water or energy consumption. To illustrate this, a breakdown of the cradle-to-gate GHG emissions for "S-DAC + Steam" scenario is also shown in Fig. 5.

A sensitivity analysis, shown in Fig. 6, was carried out analogous to the one performed in the techno-economic assessment. As already hinted by Fig. 5, the variable with the highest potential impact is the solar field surface. This variable depends strongly on the chosen location or the efficiency of the solar reactor, which may improve as the technology advances. The next variable with a higher impact is ceria consumption, expressed as a percentage of total inventory replaced on an annual basis. While an obvious interpretation of this result is that materials and reactors need to be developed to minimize structural damage to ceria structures, reducing the ceria inventory can be an equally effective countermeasure by means of higher reduction extends or lower cycle times (currently assumed to be 32 min [25]). It is also noteworthy that while the cost of water had an almost negligible impact on the LCOF, it is a relevant variable in the climate change impact category because it is obtained through desalination in a country with a high carbon intensity electricity grid.

In order to show the potential burden shifting (i.e., when one impact category is worsened at the expense of improving another), Figs. 7 and 8 have been prepared. In Fig. 7, the baseline case was set as the reference (i.e., shown as 100% for all categories) and the values for each impact category in the other scenarios were divided by the baseline and shown as a percentage. As observed, scenarios that do not use natural gas in the L-DAC achieve significantly better performance in the fossil depletion and freshwater ecotoxicity categories. Scenarios using S-DAC have a lower impact on ozone depletion because they require much less water input, which implies less plastics for the construction of desalination modules. Nevertheless, according to the LCA, S-DAC is associated with higher agricultural land use because more wood is consumed in the production of S-DAC equipment for flooring. While this may be true at a pilot scale, wood would probably not be such a relevant material for a large-scale facility, which demonstrates the general lack of high-quality primary data about DAC. Finally, it is interesting to note that the "S-DAC + HVAC" scenario requires a significant amount of electricity from PV, which translates into a higher terrestrial ecotoxicity impact due its fabrication process.

In Fig. 8, the best scenario, "S-DAC + Steam", was used as a reference (i.e., set to 100% for all categories). The values from the fossil methanol were then compared to it and expressed as percentages. Due to the large divergence in some of the impact categories, this figure was plotted on a logarithmic scale. The most favorable categories for fossil methanol are related to land use and metal depletion, as renewable energies tend to occupy more land and consume more materials. This fact, however, contrasts with the still lower impact of solar methanol in the natural land transformation category, as a high value of land transformation is associated with natural gas extraction. The results show that marine eutrophication is dominated by cerium oxide extraction, which explains the poor performance of the solar methanol pathway compared to the fossil alternative. As expected, solar methanol performs better than fossil methanol in climate change and fossil depletion impact categories.

Finally, the results of the techno-economic and environmental assessments have been combined in Fig. 9. The cost of fossil methanol was also included by using the upper range of methanol production from natural gas as reported in the literature [64]. In order to show the potential of offsetting the emissions associated with the production of

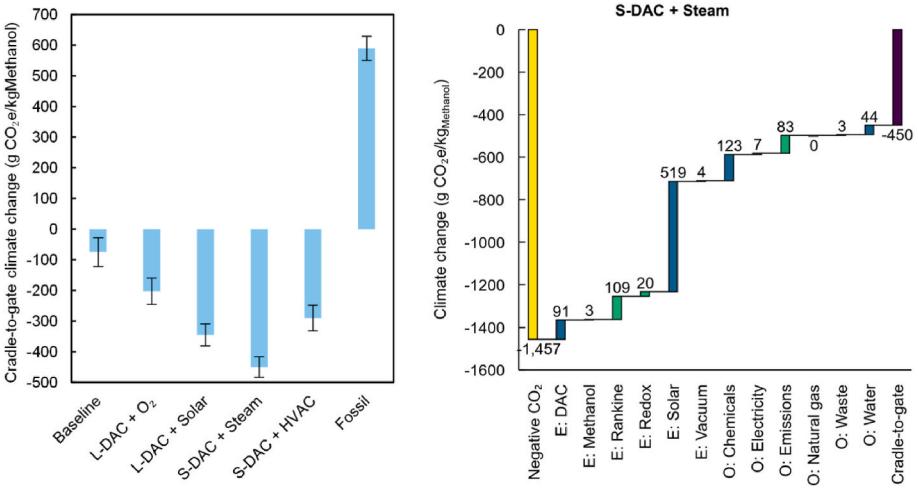

Fig. 5. On the left, climate impact category for each scenario, derived from the life cycle assessment (LCA) results with a cradle-to-gate scope. In addition, the production of methanol from natural gas is also shown with the label "fossil" to show the benchmark of conventional methanol. On the right, breakdown of climate change impact category for the "S-DAC + Steam" scenario. Categories beginning with "E" and "O" refer to embedded emissions from equipment and emissions associated with operations, respectively. Negative categories are yellow, positive categories are blue (green when equal across scenarios), and purple shows cradle-to-grave total. (For interpretation of the references to color in this figure legend, the reader is referred to the Web version of this article.)

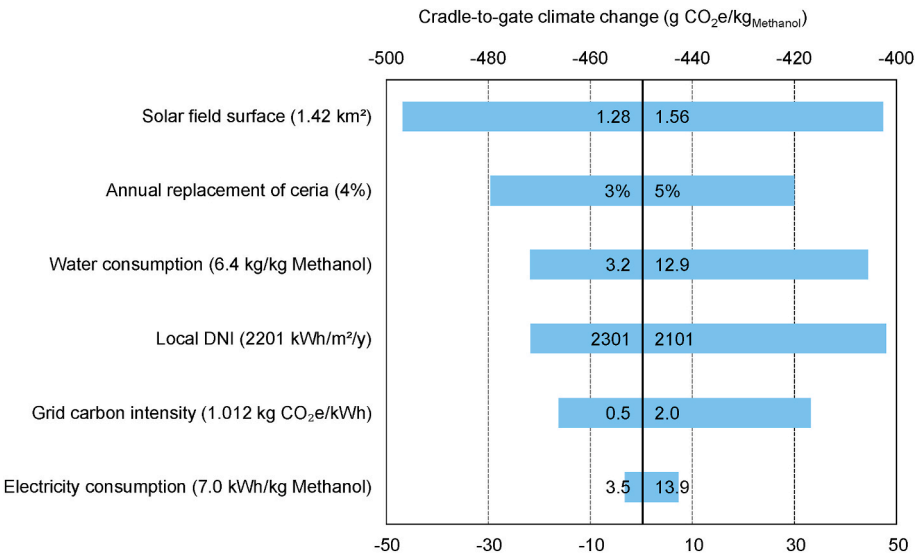

Fig. 6. Sensitivity analysis results for the "S-DAC + Steam" scenario, which has the lowest value for cradle-to-gate climate change impact category. The original value in the environmental assessment is shown in parentheses next to each variable name. The term "DNI" stands for direct normal irradiance.

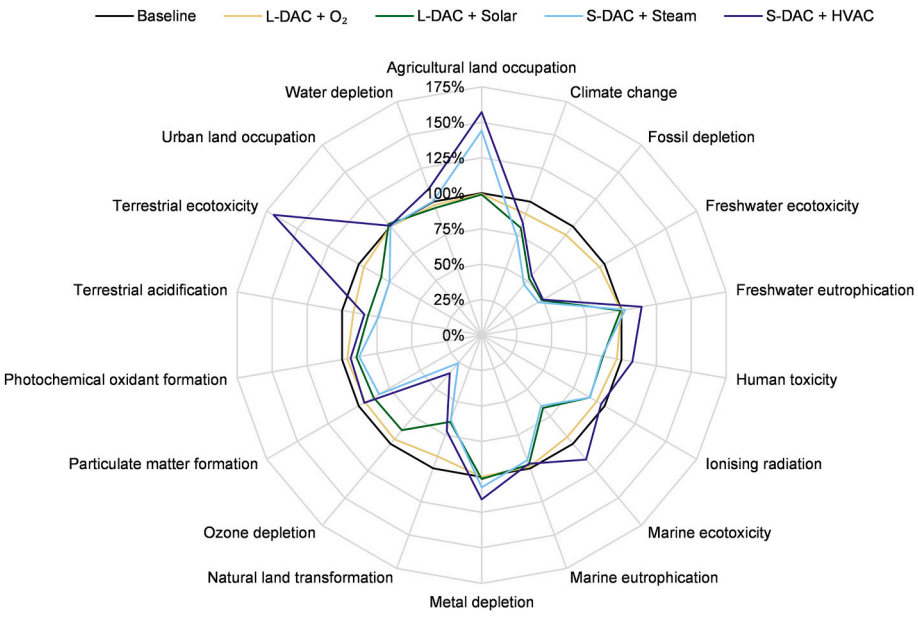

Fig. 7. Radar plot comparing all impact categories between the methanol produced in the baseline (shown as reference at 100% for all categories) and the methanol produced in the different scenarios.

methanol from natural gas, three lines have been added showing the LCOF of fossil methanol for three different costs of DAC with storage (namely 1000, 500 and 100 USD_{2022}/t CO_2 removed). Furthermore, a possible evolution of LCOF and cradle-to-gate carbon emissions is shown for the "S-DAC + Steam" scenario, which emerged as the best integration strategy from both economic and environmental perspectives. This evolution assumes that the same plant energy input leads to higher methanol outputs while keeping production costs and emissions constant. Although extremely simplistic, especially for very high system efficiencies exceeding the most optimistic predictions, Fig. 9 shows that redox cycles, with or without DAC integration, still have a long way to go to become competitive with fossil methanol, but also with synthetic methanol produced by other pathways [31–35].

It is also important to highlight that Fig. 9 compares fossil methanol production, which has decades of industrial maturity, to the proposed system, which is still far from commercial scale. For the proposed system to reach a comparable maturity, the TRL of the DAC and solar redox cycles (which currently is 7–9 [37] and 5–6 [65], respectively) must be increased. For both technologies, efficiency improvements are critical for downscaling the renewable energy infrastructure required to power them. For DAC, challenges include defossilization of the calcination step in L-DAC and development of cost-effective adsorbents for different environmental conditions. Solar redox cycles face the need to reduce CAPEX and clarify scalability, which can be addressed by developing new redox materials or reactor designs. In addition, DAC technologies are primarily targeted at large-scale CDR applications, so legislation around CDR could impact the use of captured CO_2 in carbon-neutral fuel production. Similarly, the deployment of CSP, under discussion in many national decarbonization strategies, indirectly impacts the advancement of solar redox cycles.

The threshold for carbon neutrality is also shown in Fig. 9. It is interesting to note that solar methanol is unable to reach this threshold

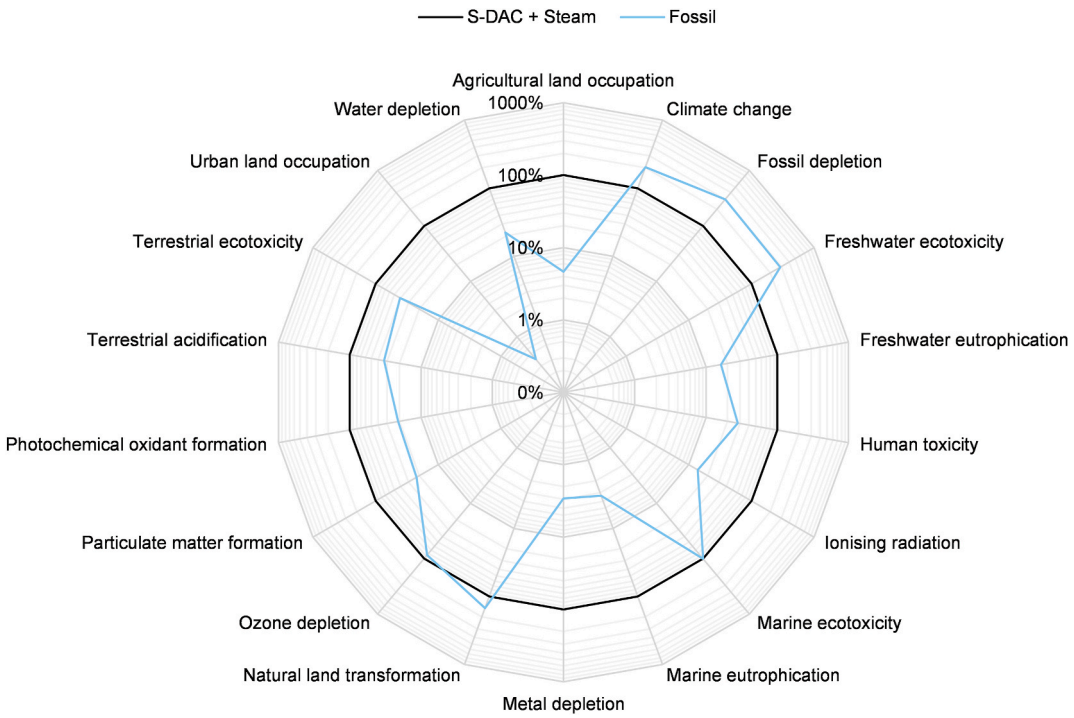

Fig. 8. Radar plot comparing all impact categories between the methanol produced in the "S-DAC + Steam" scenario (shown as reference at 100% for all impact categories) and in the fossil process. Note that the plot has a logarithmic scale.

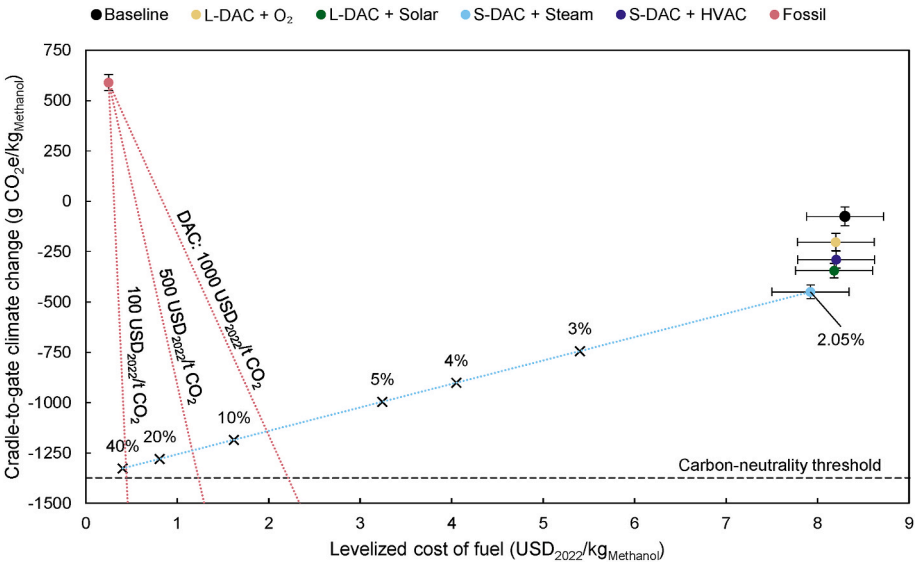

Fig. 9. Relationship between the cradle-to-gate climate change obtained from the life cycle assessment (LCA) and the levelized cost of fuel (LCOF) obtained from the techno-economic assessment for the methanol produced in each scenario and for the natural gas-based pathway. Uncertainty is shown for all scenarios for both climate change and LCOF, but for the fossil case it is only shown for climate change as its LCOF was extracted from the literature [64]. The red lines indicate the evolution of fossil methanol by offsetting CO_2 emissions with direct air capture (DAC) and storage, while the blue line indicates the potential evolution of solar methanol produced in "S-DAC + Steam" scenario when the system efficiency increases. Additionally, the minimum threshold for carbon neutrality of the produced methanol is shown as a reference. (For interpretation of the references to color in this figure legend, the reader is referred to the Web version of this article.)

even at extremely high system efficiencies. This is because the solar methanol plant is designed to capture the amount of CO_2 needed as a feedstock for methanol production. Thus, as long as there is a certain amount of GHG emissions associated with solar methanol production (which is unavoidable in practice), the fuel produced will not be completely carbon neutral. The only way to achieve a fully carbon-neutral fuel is to store a fraction of the CO_2 captured from the atmosphere to offset its production emissions. Obviously, the amount of CO_2 to be stored will be smaller for cleaner and more efficient production processes. Although beyond the scope of this study, the threshold for carbon neutrality represents only a minimum value, as aspects such as transportation and distribution of the solar methanol to the end user will add GHG emissions to the lifecycle of the fuel.

Last but not least, it is also important to mention that Fig. 9 may give the false impression that fossil fuels combined with negative emission technologies such as DAC with sequestration are more competitive than

they are, because several relevant aspects are overlooked. First, it does not take into account the evolution of the cost of fossil fuels as they become scarcer in the coming decades. Second, the availability of renewable energy sources is much more widespread than that of fossil fuels, which are concentrated in a few regions of the world, creating geopolitical tensions that have a massive impact on development. Finally, the availability, overall capacity and safety of CO_2 storage in different reservoirs is an on-going research field [66,67], and it seems reasonable to minimize the application of CCS solutions for the hardest to avoid emissions. In other words, although extracting fossil fuels, consuming them and storing the generated CO_2 may be technically possible, this is not the most efficient use of the storage capacity. Instead, producing fuels directly from CO_2 can close the carbon cycle, allowing storage capacity to be reserved for sectors with unavoidable emissions, such as cement production.

4. Conclusions

This work explores the potential integration of DAC and methanol production via a solar thermochemical cycle and shows that there are significant synergies that lead to improvements in economic and environmental terms.

A single scenario stood out as the best integration strategy from an economic and environmental perspective: the "S-DAC + Steam" scenario. This specific scenario has the most efficient energy integration because it can utilize a high fraction of the low-pressure steam produced as a by-product of the solar fuel system. Moreover, the CAPEX of the S-DAC was lower than that of the L-DAC, and combined with the lowest variable OPEX due to the small amount of water and grid electricity required to support its operation, it resulted in the most economic methanol LCOF of 7.9 ± 0.4 USD_{2022}/kg. In fact, the LCA showed that the minimal use of desalinated seawater and electricity was also highly beneficial, especially in a location with a carbon-intensive electrical grid such as Saudi Arabia. As a result, the methanol produced in the "S-DAC + Steam" scenario showed the lowest results in the climate change impact category in a cradle-to-gate scope with −450 ± 30 g CO_2e/kg.

The cost breakdown and sensitivity analysis revealed that the combined cost of chemical equipment (thermochemical cycle, methanol synthesis, vacuum system, and Rankine cycle) is the primary contributor to the LCOF for solar methanol in all scenarios. This indicates that the LCOF of solar methanol via redox cycles can be reduced by finding solutions to operate the system under milder conditions and at higher efficiencies, thus avoiding expensive materials and reducing its size. These improvements are paramount to becoming an economically competitive solution against fossil methanol, as well as synthetic methanol produced by other pathways. Conversely, the carbon footprint breakdown and sensitivity analysis points to the solar equipment as the main contributor. The environmental impact of solar methanol can therefore also be improved by achieving higher efficiencies leading to smaller solar fields (and by further decarbonizing the heliostat industry) while minimizing external energy and water inputs. In this case study, the infrastructure and operation of DAC were not the determining factors in the LCOF or carbon footprint of methanol due to the still limited efficiency of redox cycles, but their relevance is expected to increase when integrated with more mature green methanol production pathways, owing to lower costs and reduced energy consumption.

In summary, this study recommends the integration of DAC with synthetic fuel production, especially in the case of S-DAC, due to the advantages it offers in terms of waste energy utilization and reduced costs for smaller plants compared to L-DAC.

CRediT authorship contribution statement

Enric Prats-Salvado: Writing – review & editing, Writing – original draft, Methodology, Investigation, Conceptualization. **Nathalie Monnerie:** Writing – review & editing, Supervision, Project administration, Funding acquisition. **Christian Sattler:** Supervision, Project administration, Funding acquisition.

Declaration of competing interest

The authors declare the following financial interests/personal relationships which may be considered as potential competing interests: Enric Prats-Salvado, Nathalie Monnerie reports financial support was provided by Helmholtz Association of German Research Centres. If there are other authors, they declare that they have no known competing financial interests or personal relationships that could have appeared to influence the work reported in this paper.

Acknowledgements

The authors would like to thank the financial support received from DLR's Grundfinanz and the Helmholtz Climate Initiative.

Appendix A. Supplementary data

Supplementary data to this article can be found online at https://doi.org/10.1016/j.ijhydene.2024.10.026.

References

[1] United Nations Environment Programme, "Emissions gap report 2021: the heat is on - a world of climate promises not yet delivered," Nairobi, Kenya.
[2] Blunden J, Arndt DS. State of the climate in 2019. Bull Am Meteorol Soc 2020;101(8):S1–429. https://doi.org/10.1175/2020BAMSStateoftheClimate.1.
[3] Lüthi D, et al. High-resolution carbon dioxide concentration record 650,000-800,000 years before present. Nature 2008;453(7193):379–82. https://doi.org/10.1038/nature06949.
[4] Plass GN. The carbon dioxide theory of climatic change. Tellus 1956;8(2):140–54. https://doi.org/10.1111/j.2153-3490.1956.tb01206.x.
[5] International Energy Agency (IEA). Direct Air Capture: a key technology for net zero. 2022. France.
[6] Hanna R, Abdulla A, Xu Y, Victor DG. Emergency deployment of direct air capture as a response to the climate crisis. Nat Commun 2021;12. https://doi.org/10.1038/s41467-020-20437-0.
[7] Madhu K, Pauliuk S, Dhathri S, Creutzig F. Understanding environmental trade-offs and resource demand of direct air capture technologies through comparative life-cycle assessment. Nat Energy 2021;6(11):1035–44. https://doi.org/10.1038/s41560-021-00922-6.
[8] Deutz S, Bardow A. Life-cycle assessment of an industrial direct air capture process based on temperature–vacuum swing adsorption. Nat Energy 2021;6(2):203–13. https://doi.org/10.1038/s41560-020-00771-9.
[9] McQueen N, Gomes KV, McCormick C, Blumanthal K, Pisciotta M, Wilcox J. A review of direct air capture (DAC): scaling up commercial technologies and innovating for the future. Prog. Energy 2021;3(3):32001. https://doi.org/10.1088/2516-1083/abf1ce.
[10] Küng L, et al. A roadmap for achieving scalable, safe, and low-cost direct air carbon capture and storage. Energy Environ Sci 2023;16(10):4280–304. https://doi.org/10.1039/d3ee01008b.
[11] Simon B. Material flows and embodied energy of direct air capture: a cradle-to-gate inventory of selected technologies. J Ind Ecol 2023. https://doi.org/10.1111/jiec.13357.
[12] Ozkan M. Atmospheric alchemy: the energy and cost dynamics of direct air carbon capture. MRS Energy & Sustainability 2024. https://doi.org/10.1557/s43581-024-00091-5.
[13] Fasihi M, Efimova O, Breyer C. Techno-economic assessment of CO_2 direct air capture plants. J Clean Prod 2019;224:957–80. https://doi.org/10.1016/j.jclepro.2019.03.086.
[14] National Academies of Sciences, Engineering, and Medicine. Negative emissions technologies and reliable sequestration: a research agenda. 2019. https://doi.org/10.17226/25259.
[15] Marxer D, Furler P, Takacs M, Steinfeld A. Solar thermochemical splitting of CO_2 into separate streams of CO and O_2 with high selectivity, stability, conversion, and efficiency. Energy Environ Sci 2017;10:1142–9. https://doi.org/10.1039/c6ee03776c.
[16] Lu Y, Zhu L, Agrafiotis C, Vieten J, Roeb M, Sattler C. Solar fuels production: two-step thermochemical cycles with cerium-based oxides. Prog Energy Combustion Sci 2019;75. https://doi.org/10.1016/j.pecs.2019.100785.
[17] Agrafiotis C, Roeb M, Sattler C. 4.18 solar fuels. In: Dincer I, editor. Comprehensive energy systems. Amsterdam, Netherlands: Elsevier; 2018.
[18] Romero Manuel, et al., editors. Solar-driven thermochemical production of sustainable liquid fuels from H_2O and CO_2 in a heliostat field; 2019.

[19] Rytter E, et al. Process concepts to produce syngas for Fischer–Tropsch fuels by solar thermochemical splitting of water and/or CO_2. Fuel Process Technol 2016; 145:1–8. https://doi.org/10.1016/j.fuproc.2016.01.015.
[20] Bulfin B, Vieten J, Agrafiotis C, Roeb M, Sattler C. Applications and limitations of two step metal oxide thermochemical redox cycles; A review. J. Mater. Chem. A 2017;5(36):18951–66. https://doi.org/10.1039/C7TA05025A.
[21] Pein M, et al. Redox thermochemistry of Ca-Mn-based perovskites for oxygen atmosphere control in solar-thermochemical processes. Sol Energy 2020;198: 612–22. https://doi.org/10.1016/j.solener.2020.01.088.
[22] Lidor A, Bulfin B. A critical perspective and analysis of two-step thermochemical fuel production cycles. Solar Compass 2024;11:100077. https://doi.org/10.1016/j.solcom.2024.100077.
[23] Schäppi R, et al. Drop-in fuels from sunlight and air. Nature 2022;601(7891):63–8. https://doi.org/10.1038/s41586-021-04174-y.
[24] Lidor A, Aschwanden Y, Häseli J, Reckinger P, Haueter P, Steinfeld A. High-temperature heat recovery from a solar reactor for the thermochemical redox splitting of H_2O and CO_2. Appl Energy 2023;329:120211. https://doi.org/10.1016/j.apenergy.2022.120211.
[25] Weber A, Grobbel J, Neises-von Puttkamer M, Sattler C. Swept open moving particle reactor including heat recovery for solar thermochemical fuel production. Sol Energy 2023;266:112178. https://doi.org/10.1016/j.solener.2023.112178.
[26] Brendelberger S, Holzemer-Zerhusen P, Vega Puga E, Roeb M, Sattler C. Study of a new receiver-reactor cavity system with multiple mobile redox units for solar thermochemical water splitting. Sol Energy 2022;235:118–28. https://doi.org/10.1016/j.solener.2022.02.013.
[27] Prats-Salvado E, Monnerie N, Sattler C. Synergies between direct air capture technologies and solar thermochemical cycles in the production of methanol. Energies 2021;14(16):4818. https://doi.org/10.3390/en14164818.
[28] Gonzalez Sanchez R, Chatzipanagi A, Kakoulaki G, Buffi M, Szabo S. The role of direct air capture in EU's decarbonisation and associated carbon intensity for synthetic fuels production. Energies 2023;16(9):3881. https://doi.org/10.3390/en16093881.
[29] Servin-Balderas I, Wetser K, Buisman C, Hamelers B. Implications in the production of defossilized methanol: a study on carbon sources. J Environ Manag 2024;354: 120304. https://doi.org/10.1016/j.jenvman.2024.120304.
[30] Liu CM, Sandhu NK, McCoy ST, Bergerson JA. A life cycle assessment of greenhouse gas emissions from direct air capture and Fischer–Tropsch fuel production. Sustain Energy Fuels 2020;4(6):3129–42. https://doi.org/10.1039/C9SE00479C.
[31] Allgoewer L, et al. Cost-effective locations for producing fuels and chemicals from carbon dioxide and low-carbon hydrogen in the future. Ind Eng Chem Res 2024. https://doi.org/10.1021/acs.iecr.4c01287.
[32] Fulham GJ, Mendoza-Moreno PV, Marek EJ. Managing intermittency of renewable power in sustainable production of methanol, coupled with direct air capture. Energy Environ Sci 2024;17(13):4594–621. https://doi.org/10.1039/D4EE00933A.
[33] Li S, et al. Solar thermal energy-assisted direct capture of CO_2 from ambient air for methanol synthesis. npj Mater. Sustain. 2024;2(1). https://doi.org/10.1038/s44296-024-00014-y.
[34] Fasihi M, Breyer C. Global production potential of green methanol based on variable renewable electricity. Energy Environ Sci 2024;17(10):3503–22. https://doi.org/10.1039/D3EE02951D.
[35] Cameli F, Delikonstantis E, Kourou A, Rosa V, van Geem KM, Stefanidis GD. Conceptual process design and technoeconomic analysis of an e-methanol plant with direct air-captured CO 2 and electrolytic H 2. Energy Fuels 2024;38(4): 3251–61. https://doi.org/10.1021/acs.energyfuels.3c04147.
[36] Prats-Salvado E, Monnerie N, Sattler C. Techno-economic assessment of the integration of direct air capture and the production of solar fuels. Energies 2022;15 (14):5017. https://doi.org/10.3390/en15145017.
[37] Bisotti F, Hoff KA, Mathisen A, Hovland J. Direct Air capture (DAC) deployment: a review of the industrial deployment. Chem Eng Sci 2024;283:119416. https://doi.org/10.1016/j.ces.2023.119416.
[38] Dittmeyer R, Klumpp M, Kant P, Ozin G. Crowd oil not crude oil. Nat Commun 2019;10. https://doi.org/10.1038/s41467-019-09685-x.
[39] Keith D, Holmes G, Angelo D St, Heidel K. A process for capturing CO_2 from the atmosphere. Joule 2018;2:1573–94. https://doi.org/10.1016/j.joule.2018.05.006.
[40] Sendi M, Bui M, Mac Dowell N, Fennell P. Geospatial analysis of regional climate impacts to accelerate cost-efficient direct air capture deployment. One Earth 2022; 5(10):1153–64. https://doi.org/10.1016/j.oneear.2022.09.003.
[41] An K, Farooqui A, McCoy ST. The impact of climate on solvent-based direct air capture systems. Appl Energy 2022;325:119895. https://doi.org/10.1016/j.apenergy.2022.119895.
[42] Prats-Salvado E, Jagtap N, Monnerie N, Sattler C. Solar-powered direct air capture: techno-economic and environmental assessment. Environ Sci Technol 2024. https://doi.org/10.1021/acs.est.3c08269.
[43] Schwarzbözl P, Pitz-Paal R, Schmitz M, editors. Visual HFLCAL - a software tool for layout and optimisation of heliostat fields; 2009.
[44] Bulfin B, et al. Thermodynamics of CeO_2 thermochemical fuel production. Energy Fuels 2015;29:1001–9. https://doi.org/10.1021/ef5019912.
[45] Albrecht KJ, Ho CK. Heat transfer models of moving packed-bed particle-to-SCO_2 heat exchangers. In: ASME 2017 11th international conference on energy sustainability, charlotte, North Carolina, USA; 2017.
[46] Albrecht KJ, Ho CK. "High-temperature flow testing and heat transfer for a moving packed-bed particle/sCO_2 heat exchanger,". 2018, 40003. Santiago, Chile.
[47] Albrecht KJ, Ho CK. Design and operating considerations for a shell-and-plate, moving packed-bed, particle-to-sCO_2 heat exchanger. Sol Energy 2019;178: 331–40. https://doi.org/10.1016/j.solener.2018.11.065.
[48] Falter C, Pitz-Paal R. Energy analysis of solar thermochemical fuel production pathway with a focus on waste heat recuperation and vacuum generation. Sol Energy 2018;176:230–40. https://doi.org/10.1016/j.solener.2018.10.042.
[49] Brendelberger S, von Storch H, Bulfin B, Sattler C. Vacuum pumping options for application in solar thermochemical redox cycles – assessment of mechanical-, jet- and thermochemical pumping systems. Sol Energy 2017;141:91–102. https://doi.org/10.1016/j.solener.2016.11.023.
[50] Ullmann's encyclopedia of industrial chemistry. Weinheim, Germany: Wiley-VCH Verlag GmbH & Co. KGaA; 2000.
[51] Sollai S, Porcu A, Tola V, Ferrara F, Pettinau A. Renewable methanol production from green hydrogen and captured CO_2: a techno-economic assessment. J CO2 Util 2023;68:102345. https://doi.org/10.1016/j.jcou.2022.102345.
[52] Säck J-P, et al. High temperature hydrogen production: design of a 750 KW demonstration plant for a two step thermochemical cycle. Sol Energy 2016;135: 232–41. https://doi.org/10.1016/j.solener.2016.05.059.
[53] Buck R. G3P3 techno-economic analysis of up-scaled CentRec® receiver. German aerospace center (DLR) institute of solar research, cologne. 2021.
[54] Buck R, Sment J. Techno-economic analysis of multi-tower solar particle power plants. Sol Energy 2023;254:112–22. https://doi.org/10.1016/j.solener.2023.02.045.
[55] Institute for Advanced Sustainability Studies (IASS) and others, Concentrating Solar Power Projects. [Online]. Available: https://solarpaces.nrel.gov/(accessed: June 2022).
[56] Trieb Franz, Schillings Christoph, O'Sullivan Mariene, Pregger T, editors. Global potential of concentrating solar power; 2009.
[57] Peters MS, Timmerhaus KD, West RE. Plant design and economics for chemical engineers. fifth ed. Boston, London: McGraw-Hill; 2003.
[58] Remer DS, Chai LH. Process equipment, cost scale-up. New York: Marcel Dekker, Inc.; 1993.
[59] Ameli N, et al. Higher cost of finance exacerbates a climate investment trap in developing economies. Nat Commun 2021;12(1):4046. https://doi.org/10.1038/s41467-021-24305-3.
[60] Huijbregts M, et al. ReCiPe 2016 v1.1: a harmonized life cycle impact assessment method at midpoint and endpoint level. The Netherlands: Bilthoven; 2017.
[61] Ng RT, Hassim MH, Hurme M. A hybrid approach for estimating fugitive emission rates in process development and design under incomplete knowledge. Process Saf Environ Protect 2017;109:365–73. https://doi.org/10.1016/j.psep.2017.04.003.
[62] Telsnig T. Standortabhängige Analyse und Bewertung solarthermischer Kraftwerke am Beispiel Südafrikas. Institut für Energiewirtschaft und Rationelle Energieanwendung. Stuttgart, Germany: Universität Stuttgart; 2015. Doctoral Thesis.
[63] Bruhn T, Naims H, Olfe-Kräutlein B. Separating the debate on CO_2 utilisation from carbon capture and storage. Environ Sci Pol 2016;60:38–43. https://doi.org/10.1016/j.envsci.2016.03.001.
[64] International Renewable Energy Agency (IRENA) and the Methanol Institute. Innovation outlook: renewable methanol. Abu Dhabi: International Renewable Energy Agency; 2021.
[65] Zoller S, et al. A solar tower fuel plant for the thermochemical production of kerosene from H_2O and CO_2. Joule 2022;6(7):1606–16. https://doi.org/10.1016/j.joule.2022.06.012.
[66] Snæbjörnsdóttir SÓ, Sigfússon B, Marieni C, Goldberg D, Gislason SR, Oelkers EH. Carbon dioxide storage through mineral carbonation. Nat Rev Earth Environ 2020; 1(2):90–102. https://doi.org/10.1038/s43017-019-0011-8.
[67] Kearns J, et al. Developing a consistent database for regional geologic CO_2 storage capacity worldwide. Energy Proc 2017;114:4697–709. https://doi.org/10.1016/j.egypro.2017.03.1603.